NTU Journal of Engineering and Technology (2026) 5 (1) : 105-120
DOI: https://doi.org/10.56286/ntujet.v5i1

IRAQI Academic Scientific Journals

P-ISSN: 2788-9971 E-ISSN: 2788-998X
NTU Journal of Engineering and Technology
Available online at: https://journals.ntu.edu.iq/index.php/NTU-JET/index

Performance Evaluation of a Hybrid PVT-ST System under the Influence of Dual Water Flows and a Single Airflow Velocity

Omar Younis Hamada[1] Omar Rafee Al omar[1]
1 Northern Technical University/ Mosul Technical Engineering College
M.S. student / Northern Technical University / Mosul Technical Engineering College
omar_younis@ntu.edu.iq, omar.alomar@ntu.edu.iq

Article Informations

Received: 03-05- 2025,
Revised: 11-12-2025
Accepted: 22-12-2025,
Published online: 22-03-2025

Corresponding author:
Name: Omar Younis
Affiliation : Northern Technical University
Email: omar_younis@ntu.edu.iq

Key Words:
Investigation, Performance, Connected, Photovoltaic Thermal Collector, Solar thermal Collector

A B S T R A C T

Solar thermal (ST) collectors are an efficient technology for generating thermal energy without the need for an electrical source, unlike photovoltaic thermal (PVT) collectors, which combine photovoltaic and thermal conversion to produce electricity and low-grade thermal energy. This research aims to present a low-cost strategy for improving the dual performance of PVT and ST systems by connecting them in series, under operating conditions that include different water flow rates and constant air flow in the ST unit. This work evaluates the thermal and electrical performance of a hybrid (PVT-ST) system, focusing on the effect of incorporating porous media and phase change materials (PCMs) into the system design. The results demonstrate that the integrated system enhances the heating efficiency of both water and air, contributing to an increase in the overall energy production efficiency. Experimental data showed that decreasing the water flow rate increased temperatures, while increasing the flow reduced temperature fluctuations and improved thermal production. The highest water temperature difference in the PVT system was recorded at 15.9°C at the lowest water flow, and the highest outlet air temperature was 58.5°C under the same conditions. The PVT-ST system's maximum total thermal power output was 756.13 W, achieving an overall thermal efficiency of 110.6%, an electrical efficiency of 12.22%, and a maximum electrical output of 142.69 W. The integration of thermal energy storage technologies enhances the stability of the system's performance, especially during periods of low solar radiation. The use of porous media improves internal heat transfer and distribution, while phase change materials help store and gradually release thermal energy, reducing temperature fluctuations and enhancing the stability and efficiency of the thermal and electrical systems.

Introduction

Renewable energy sources provide a feasible method for attaining enduring energy sustainability. They present various advantages, such as being eco-friendly and limitless [1]. Solar energy is acknowledged as a precious, affordable, and green resource [2][3]. In recent times, solar power plants have been widely used for electricity generation due to their low capital costs, which has driven significant growth in this sector. The two main methods for converting solar energy into electricity are photovoltaic (PV) systems and concentrated solar power (CSP) systems [4]. The integration of PV collectors with various systems, such as air and water heating systems, is crucial for energy production [5]. One such device is the flat-plate solar thermal (ST) collector, designed to convert solar radiation into thermal energy, primarily for producing hot water. With its simple and effective design, it serves both residential and industrial applications. This straightforward approach not only simplifies maintenance but also enhances cost-effectiveness [6]. A (PV) apparatus functions by converting solar radiation directly into electrical energy [7]. In addition, in photovoltaic (PV) systems, most of the solar energy is wasted as heat, with only a small fraction being converted into electricity. This limitation inspired engineers to develop photovoltaic–thermal (PVT) systems, which are designed to simultaneously capture solar energy for both thermal and electrical power production [8]. Water or air is primarily used as the working fluid in PVT systems. The fluid flows through channels located on the back of the solar panels to reduce panel temperatures and increase electrical output. Additionally, this setup produces moderately hot water. The thermal performance of ST collectors has been enhanced through numerous research studies. Both active and passive methods are employed to improve thermal performance, with passive methods mainly enhancing the heat transfer properties of the absorber tube. Phase-change material (PCM) technology has also been applied to further improve energy storage and thermal efficiency [9], PM [10]. In the mid-1970s, Wolf and colleagues proposed the novel concept of the photovoltaic–thermal (PVT) module. This invention is based on the principle that PV modules and solar collectors can absorb energy from different bands of the solar spectrum. The solar PV/T module is a device that combines the functions of a solar collector and a PV module to generate both electrical and thermal energy simultaneously [11]. However, the PV/T module is significantly constrained by the PV module covering the absorber plate. This configuration leads to high operating temperatures in the PV module, which prevents a large portion of the incoming solar radiation from directly reaching the heat exchanger beneath the plate. Consequently, the system can only generate low-temperature thermal energy (commonly below 40.0°C). This limitation is a key factor hindering the advancement of PVT modules [12]. Recent research has investigated the integration of (PVT) and (ST) systems, collectively termed PVT-ST. The objective of these investigations is to address the problem of reducing the PVT system's output temperature and raising the ST system's output temperature. Kazemian et al [13] A comparative study was conducted utilizing four distinct hybrid nanofluids alongside a PVTST module. In comparison to the other nanofluids evaluated, the computational analysis revealed that the nanofluid made of multiwall carbon and silicon carbide demonstrated the greatest thermal efficiency, reaching a value of 56.55 %. Ma et al. [14] developed the PVT-ST integrated system to address the challenges of low output temperatures in PVT modules and the limited electricity generation in ST systems. The researchers first assessed the feasibility of this novel technology and created a stable system, whose thermal and electrical performance was analyzed using a two-dimensional (2D) model. The analysis demonstrated that the PVT-ST system has a minimal effect on electrical efficiency while producing high-quality thermal energy. Consequently, it achieves a high level of energy-saving efficiency. Li et al [15] SA transient 2D model was created to A transient 2D SA model was created to conduct a numerical simulation of four scenarios involving a PVT–ST system, considering both glazed and unglazed configurations. This study aimed to enhance the performance of the individual PVT and ST modules. The findings indicated that Scenario 1, which included the glazed PV/T and glazed ST units and achieved the highest overall energy and exergy efficiencies, recorded efficiencies of 41.51% and 17.63%, respectively. Salman et al [16] evaluated a novel design of a PV panel cooling system aimed at improving performance by lowering the panel temperature. Water was used as a coolant flowing through a back chamber equipped with a porous medium to enhance convective heat transfer. The results indicated that incorporating the porous medium reduced the average panel temperature by 9–14 °C, while increasing the flow rate significantly improved heat transfer. Han et al. [17] compared the performance of two systems: a standalone PV system integrated with an ST module and a PVT system connected in series with an ST module. Using a heat-transfer model, the study evaluated the electrical, thermal, and total efficiencies of both configurations under various environmental conditions. The analysis showed that the PV–ST system provides greater primary energy-saving efficiency at lower ambient temperatures and lower solar irradiance levels, whereas the PVT–ST system

performs better under high ambient temperatures and high solar radiation intensity. Menon et al [18] investigated the effect of using nanofluid and water on the electrical and thermal performance of an unglazed PVT system. The experimental results indicated that water cooling reduced the cell temperature by 15 °C, while using nanofluid it decreased by 23.7 °C and the electrical efficiency increased by 14.58% and 17.61% for water and nanofluid, respectively. Moreover, the thermal efficiency of the system increased by 58.77% for water and 71.71% for nanofluid, with an initial energy-saving efficiency of 117.53% versus 97.15% for water, confirming the effectiveness of nanofluid in improving the performance of PVT systems. Suresh et al [19]. examined a (PVT) system linked to an (ST). A three-dimensional numerical model was developed for both glazed and unglazed PVT-ST collectors to evaluate their performance. Research on the unglazed PVT-ST collector indicated a maximum outlet water temperature of 63 °C at a flow rate of 0.5 liters per minute (LPM). The ST collector demonstrated a thermal efficiency of 35%, while the unglazed PVT collector exhibited peak electrical and thermal efficiencies of 16% and 25%, respectively. In contrast, glazed PVT-ST collectors reached peak outlet water temperatures of 67 °C at the same flow rate of 0.5 LPM. Alikhan et al [20] evaluated energy and exergy within a 3D transient numerical simulation of series-connected (PVT) and (ST) systems that incorporate PCM(PCMs). The performance of the proposed system was compared to a configuration lacking PCM at various mass flow rates of the heat transfer fluid. Findings indicated that PCMs influence the temperature of PV cells, leading to enhancements in both power output and exergy. While an increase in mass flow rate enhances electrical and thermal power, it simultaneously reduces thermal exergy. Altharwanee et al [21] investigated and compared PVT and ST systems, PVT-ST under different Weather patterns, analyzed on four consecutive days of January, February, March and April. The results of the study demonstrated that the PVT-ST system improved hot water temperature yield compared to those with ST alone. Temperature changes of (6.15, 6.65, 7.51, and 5.48) ◦C were observed during four testing days. Compared to the ST system, the PVT-ST system enhanced thermal efficiency by 24.80%, 18.20%, 22.30%, and 19.4% over four testing days. The mean exergy efficiency rose 7.98%, 7.45%, 7.82%, and 6.97%. In four days, the PVT system increased electricity efficiency by 31.04%, 41.16%, 47.34%, and 11.55% compared to PV panels. However, there are limited reports on experimental investigations of integrated PVT systems combined with solar thermal collectors, in addition to a small number of studies comparing the serial integration of PVT units with ST units—referred to as PVT-ST systems—which have been shown to enhance operational performance compared to standalone units. As is well known, Iraq suffers from significant electricity waste due to oil combustion, resulting in substantial financial expenditures. However, it possesses enormous potential for utilizing solar energy in power generation and heating applications. To address this challenge, an integrated system combining a photovoltaic thermal (PVT) module and a ST system represents one of the most effective solutions for such year-round applications and can be implemented in many regions worldwide facing electricity generation challenges. Thus, a PVT-ST system can support power plants. Based on the preceding discussion, no studies have been published integrating a water-based thermal collector with an air-water ST module equipped with porous media (PM) and phase change materials (PCM) within the module. This integration aims to generate electricity and hot water from the PVT system, while the ST module provides hot water and hot air. Therefore, the scientific objective of this study is to evaluate the performance of this hybrid PVT-ST system, analyze the effect of integrating PCM and PM on the thermal performance of the system, examine the effect of changing the water flow rate on operational efficiency, and use PCM and PM to improve thermal storage and heat transfer.

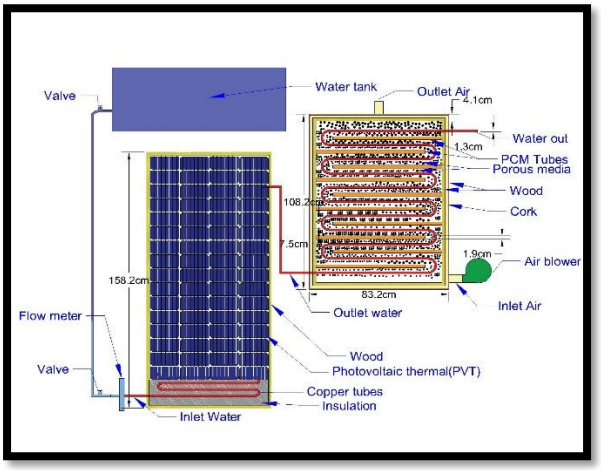

(a)

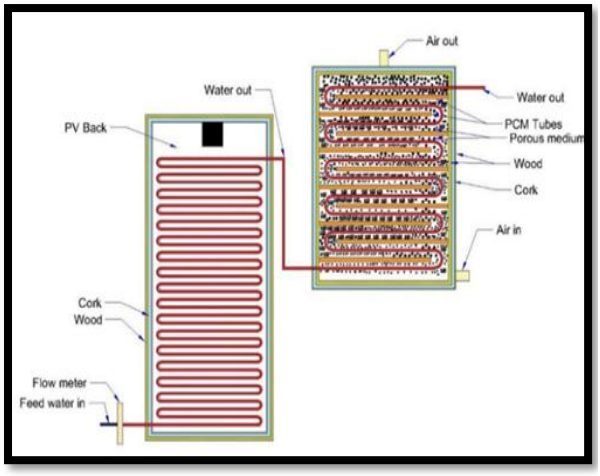

(b)

Fig.1. Illustrative diagram of the PVT-ST module: (a) Dimensions and labeled components of the module; (b) Overall configuration of the PVT–ST module.

1.1.2. Configuration of the PVT

The (PVT) system employed in this study consists of a (PV) module integrated with a spiral-shaped heat exchanger composed of 34 copper tubes. Each tube has a length of 630 mm, an outer diameter of 12.7 mm, and a wall thickness of 0.710 mm. The tubes are arranged 25 mm apart to ensure uniform heat distribution and to maximize the contact surface between the absorber and the PV cells, which enhances both the thermal and electrical performance of the system. The spiral configuration of the copper tubes improves the fluid flow path and increases the heat transfer rate between the cooling medium and the PV panel surface. To ensure effective thermal contact, The heat exchanger is carefully installed on the back surface of the solar PV module using locally available silicone gel. This industrial silicone is characterized by its low thermal conductivity, ranging between 0.2 and 0.35 W/m·K, making it an effective thermal insulator suitable for applications that require minimizing heat transfer. Cork sheets, aluminum straps, and a wooden box are used to secure and support the heat exchanger. Cork acts as an efficient thermal insulator, significantly reducing heat losses to the surrounding environment and consequently enhancing the system's thermal efficiency. All components of the PVT system are installed inside a wooden enclosure to minimize heat dissipation and to protect the assembly from environmental factors such as dust, humidity, and wind. Table 1 presents the detailed specifications and operational parameters of the system components. This integrated design effectively balances electrical power generation and thermal energy recovery, demonstrating the system's strong potential for implementation in renewable energy and hybrid solar applications, particularly in regions characterized by high solar radiation, such as the city of Mosul.

Table 1. The PVT system's dimensions and specifications.

Components	Factors	Values
PV panel	Area (length × width)	1.1m²(1550*710 mm)
	Maximum Power (Pmax)	200 W
	Open-Circuit Voltage (Voc)	21V
	Short-Circuit Current (Isc)	11.78A
	Voltage at Pmax (Vmp)	18V
	Current at Pmax (Imp)	11.11A
	Power Tolerance	+/-3%
Insulation Wood	Area	1.22m²
	Thickness	16mm
Crok	Area	1.1 m²
	Thickness	20 mm
Absorber Copper tube	Outer diameter/Inside	1.128mm/1.27mm
	Number of tubes	34
	Thermal conductivity	394 w/ (m.k)

1.1.3. Configuration of the ST

A ST solar collector (air-water) with a total area of 0.75 m², includes an absorber plate, glass cover and several tubes is considered. It is composed of ten paraffin wax filled tubes which have also an outer diameter of 1.93 cm and are interspersed between the heat exchanger tubes in the exchanger space to improve thermal storage as well as heat transfer. The features of paraffin wax for the system are listed in Table 2, for the gravel porous medium used to enhance heat transfer inside ST is shown as well (Table 3). Furthermore, in the ST, a spiral heat exchanger consisting of 11 copper tubes (1.27 cm outer diameter) separated by 7 cm and filled with a porous medium layer of thickness h = 3 cm is

employed. The heat exchanger is assembled on top of the PM, with (PCM) tubes between the heat exchanger tubes in such a manner that thermal interaction is possible between the heat exchanger and the storage. Furthermore, an air blower blows ambient air into the solar thermal collector to improve convective heat transfer in the system. Water flows into the ST collector from the outlet of the (PVT) collector, allowing its integration with the hybrid system and utilization of PVT unit's recovered thermal energy. This design enables concurrent heating of the air and water flow, taking advantage of the thermal storage by PCM and PM.

Table 2. Thermophysical properties of paraffin wax.[22][23][24]

Properties/Unit	Values
Melting temperature, °C	54-57
Liquid specific heat, kJ/kg. °C	2.15
Solid specific heat, kJ/kg. °C	2
Thermal conductivity, W/m. °C	0.22
Solid density, kg/m³	910
Liquid density, kg/m³	790
Expanding volume due to a change in phase from solid to liquid, %	0.15
Latent heat of fusion, kJ/kg	170
Paraffin wax weight for ten circular pipes as a whole, g	1100

Table 3 Specifications and numbers of porous materials[3][22]

Type of porous medium	Number of samples(depth)	Thermal conductivity W/m· K	Heat capacity J/kg· °C	Porosity (%)
Stones	7317	0.520	184.0	45

1.2. Description of the Experimental Setup.

The experimental investigation was conducted in Mosul City, located at a latitude of 36.32°N and a longitude of 43.15°E. The system consisted of a hybrid photovoltaic–thermal and solar thermal collector (PVT-ST) mounted on a steel platform designed for structural stability, with an adjustable tilt angle of 47°. The system was oriented southward to maximize solar radiation exposure and included essential components such as structural supports, plumbing, a water storage tank, and auxiliary equipment. This configuration was carefully selected to replicate real-world operating conditions, thereby enhancing the practical relevance of the experimental results. As shown in Figure 2, which also illustrates the locations of the temperature and flow sensors installed throughout the system, measurements were recorded at 30-minute intervals using the AT 4208 device. Table 5 summarizes the operational specifications of the measurement instruments used in the system. In the operation process, water was pumped from storage tank and introduced to PVT unit where it was preheated. The preheated water was then sent to the ST unit for additional heating and stored in the last tank. This tandem approach maximizes the use of thermal energy whereby the PVT collector used for pre-heating, followed by the ST unit for additional energy absorption—to achieve enhanced thermal efficiency. The alignment of the PVT outlet with the ST inlet ensured effective heat transfer across the system. The experiment was conducted over two clear days in February and March 2025, during which the water mass flow rate was varied at four distinct levels, while the airflow rate in the air–water ST system remained constant. This experimental methodology demonstrates a commitment to maximizing solar energy utilization and provides valuable insights into the dynamic performance of the PVT-ST system under varying operational conditions

Table 4 Measurement range of the devices and accuracy

Devices	Specifications	Range	Accuracy
Solar meter	SURVEY100	100-1250 W/m²	± 0.85 W/m²
Thermocouple	K-type	−200 ~ 1300° C	± 0.2°C
Multi-function data logger	AT 4208	/	/
Anemometer	UT363BT	0-30 m/s	± 0.35 m/s
Flowmeter	SHLLJ	0.1-2L/m	± 2.5%
Digital Multimeter Voltage Current	DT9205A DC DC	200m V-1000V 2mA-20A	±0.8% ±1%

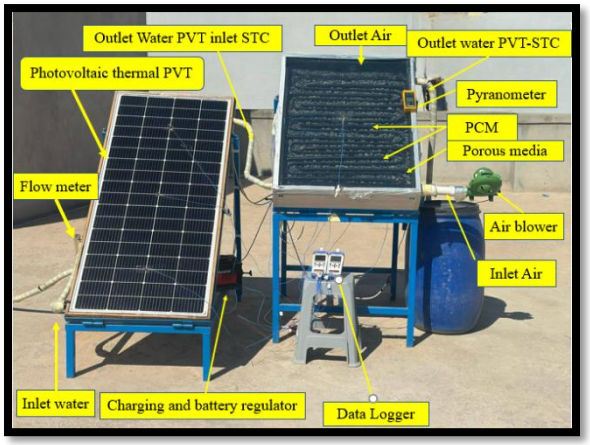

Fig.2. Photograph of the experimental PVT–ST system setup.

2. Performance analysis

It is necessary to address the electrical efficiency of the system. The power conversion efficiency of a PV module is defined as the ratio of its electrical output to the amount of incident solar radiation it receives, as illustrated by the following equation(1)[27].

$$\eta_{\text{ele}} = \frac{P}{GA_{PV}} = \frac{VI}{GA_{PV}} \quad (1)$$

P indicates the electrical power produced, while G represents the solar power received by the PV module, A_{PV} denotes the surface area of the PV module ,and$V$ and I , refer to the voltage and current generated by the PV, respectively. The maximum power output $\boldsymbol{P}_{\text{max}}$extracted from the PVT system is obtained when the output voltage $\boldsymbol{V_{mp}}$, and a current $\boldsymbol{I_{mp}}$ correspond to the maximum power point of the PV module, at which the electrical resistance is optimal. Equation (2) is used for this calculation[28]

$$\boldsymbol{P}_{\text{max}} = \boldsymbol{V_{mp}} \times \boldsymbol{I_{mp}} \quad (2)$$

The fill factor$\boldsymbol{FF}$ of a solar cell is defined as the ratio of the maximum obtainable power to the product of the open-circuit voltage($\boldsymbol{V_{oc}}$) and the short-circuit current ($\boldsymbol{I_{sc}}$), It can be calculated using the following equation(3).[29]

$$\boldsymbol{FF} = \frac{P_{\text{max}}}{V_{oc} \times I_{sc}} \quad (3)$$

The fill factor is measured under standard test conditions, with a solar irradiance of 1000 W/m² and an ambient temperature of 25 °C, to determine the optimal peak efficiency of photovoltaic (PV) systems. Consequently, it serves as a key metric for assessing the manufacturing quality of solar cells. The performance decreases by approximately 0.01% per Kelvin as the cell surface temperature increases[30].

The thermal energy of ST and PVT in the water systems may be calculated from the following equation (4).[31]

$$\boldsymbol{Q_w} = \dot{\boldsymbol{m}}\boldsymbol{Cpw}(\boldsymbol{T}_{\text{wo}} - \boldsymbol{T_{win}}) \quad (4)$$

where $\dot{\boldsymbol{m}}$ is the water mass flow rate, $\boldsymbol{Cpw}$ is the specific heat capacity of water, and $\boldsymbol{T}_{\text{wo}}$,and $\boldsymbol{T_{ai}}$are the outlet and inlet water temperatures, respectively. The thermal efficiency of a solar thermal (ST) system for air applications can be calculated using the following equation(5)[32].

$$\boldsymbol{Q_a} = \dot{\boldsymbol{m}}\boldsymbol{Cpa}(\boldsymbol{T}_{\text{ao}} - \boldsymbol{T_{ai}}) \quad (5)$$

where $\dot{\boldsymbol{m}}$ is the mass flow rate, $\boldsymbol{Cpa}$ is the specific heat, $\boldsymbol{T}_{\text{ao}}$ Is the exit temperature and $\boldsymbol{T_{ai}}$is the inlet temperature of the air. The air mass flow rate $\dot{\boldsymbol{m}}$ can be calculated by the following equation (6).

$$\dot{\boldsymbol{m}} = \boldsymbol{\rho V_d A_d} \quad (6)$$

The cross-sectional area of the outlet duct is represented by $A_d = \frac{\pi}{4}d^2$

The effective heat gained from the hybrid collector is calculated by summing the heat absorbed by both the water and the air, as indicated in the following equation(7).[33].

$$\boldsymbol{Q_u} = \boldsymbol{Q_a} + \boldsymbol{Q_w} \quad (7)$$

The thermal efficiency of the PVT and the ST collectors can be found from the following equation (8):

$$\boldsymbol{\eta_{th}} = \frac{Q_a}{GA_{ST}} = \frac{Q_w}{GA_{ST,PVT}} = \frac{Q_u}{GA_{ST}} \quad (8)$$

The thermal efficiency of the PVT-ST module can be found from the following equation (9) [34-35]:

$$\boldsymbol{\eta_{th}} = \frac{\dot{Q}_{th}}{G \cdot (A_{PVT} + A_{STC})} \quad (9)$$

where A denotes the absorber area in the (ST) system and the (PV) area in the (PVT) system.

2.1. Uncertainty Analysis

The largest uncertainties of the calculated and measured quantities for the PVT-ST system are obtained as follows[36]:

$$w_\tau = \left[\left(\frac{\partial Z}{\partial x_1} w_1\right)^2 + \left(\frac{\partial Z}{\partial x_2} w_2\right)^2 + \cdots + \left(\frac{\partial Z}{\partial x_n} w_n\right)^2\right]^{\frac{1}{2}} \quad (10)$$

where w_τ, x_1, …, x_n, w_1, …, w_n and Z represent the total uncertainty, the independent variables, the uncertainties in the independent variables, and the calculated function, respectively. The uncertainties in, T_{wo} , T_{ao} , $\dot{m}_a$, $\dot{m}_w$ and η_{th} are equal ±3.45%, ±4.10%,±0.020%,±0.025%,and±5.6%, respectively.

3- Results and Discussion:

3.1. Experimental parameters

Tests on the air-to-water PVT-ST were performed in Woburn during February and March 2025 for different operating conditions. Two water mass flow rates—0.00333 kg/s and 0.00583 kg/s—were tested on February 25 and March 1, respectively, while maintaining a constant air mass flow rate of 0.007065 kg/s in the ST collector for both test days. As can be seen in Figure (3), the solar radiation that was received during both experiments was fairly constant from day to day. The tests were conducted between 9:00 a.m. and 5:00 p.m., and the maximum solar irradiance values recorded were 1078 W/m² and 1061 W/m² on February 25 and March 1, respectively, at 12:30 p.m. Solar irradiance increased gradually in the morning, peaked at noon, and then decreased steadily in the afternoon. As the outlet water temperature decreased the water-cooling system was switched off at 5 p.m. to avoid interfering with the collector performance after the interruption of solar radiation. At this point, the PVT collector began to cool the water instead of heating it. Meanwhile, the air subsystem continued operating until 8:30 p.m., benefiting from the extended heat retention provided by the thermal storage media (TSM) within the ST collector. This storage consisted of PCM(PCMs) such as paraffin wax and PM(PMs) such as gravel, which effectively prolonged heat retention during evening hours.

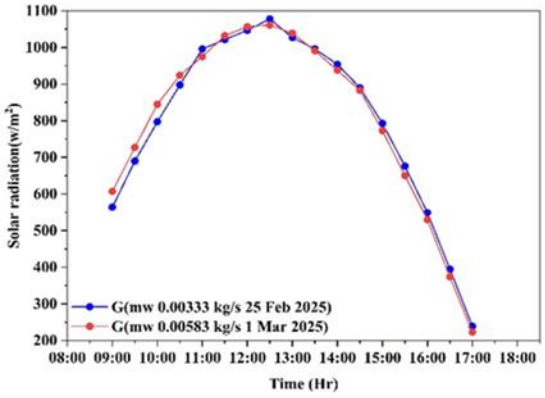

Fig. .3. Variation in solar radiation intensity for four-day experiments (25 Feb,1 Mar 2025).

3.2. Water Outlet Temperature

Water preheating through the photovoltaic–thermal (PVT) collector significantly enhances the overall thermal performance of the system under various operating conditions. In the PVT-ST configuration, the outlet temperature of the PVT collector is equivalent to the inlet temperature of the solar thermal (ST) collector, allowing the ST unit to begin operation with preheated rather than ambient water. This process increases the thermal efficiency of the system and results in a notable rise in outlet water temperature. As illustrated in Figure 4, the profiles of inlet, outlet, and ambient water temperatures for both the PVT and ST collectors indicate that the temperature of the combined PVT-ST system peaks shortly after 1:00 p.m. The preheating mechanism not only improves the thermal efficiency but also enhances the system's heat storage capability, leading to a gradual increase in outlet water temperature during the later operating hours. This improvement is further supported by the thermal storage elements integrated into the air–water ST collector, which consist of PCM such as paraffin wax, and (PMs) such as gravel. These materials absorb and store heat when solar intensity is high and release it slowly as solar irradiance decreases. Consequently, the outlet water temperature from the ST collector is relatively low in the morning but rises progressively throughout the day due to the release of stored heat under low irradiance conditions. Experimental observations also revealed that variations in the water mass flow rate had a significant impact on the outlet water temperature. Higher flow of water resulted in lower outlet temperatures due to the shorter dwell time of the water inside collectors, allowing for more effective heat absorption. At 1:00 p.m., the temperature differences across the PVT collector were 15.9°C and 11.8°C for flow rates of 0.00333 kg/s and 0.00583 kg/s, respectively. The ST collector

recorded its maximum temperature differences at 1:30 p.m., reaching 14.2°C and 11.9°C for the same flow conditions. The evening variations in the outlet temperature of the ST collector can be attributed to the excellent heat-retaining capacity of the PCM and PM materials, which enable the system to maintain elevated water temperatures even after the decline of solar irradiance.

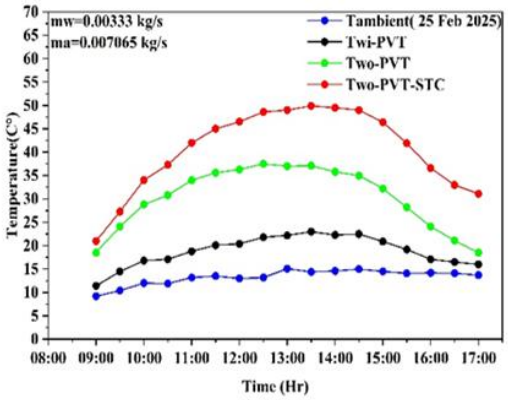

(a)

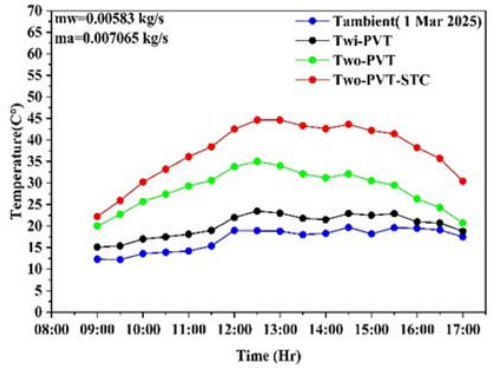

(b)

Fig.4. Surrounding temperature, water outlet temperature, and water inlet temperature of the PVT-ST system. (a) at a water mass flow rate of 0.00333kg/s (25 Feb 2025). (b) at a water mass flow rate of 0.00583 kg/s (1 Mar 2025)

3.3. Air Outlet Temperature

The results indicate that water flow rates have a limited impact on the outlet air temperature of the ST system. At lower water flow rates, the outlet air temperature increases due to the longer thermal contact time with the water and heat storage media, while the air mass flow rate remained constant at 0.007065 kg/s. Figure 5a shows the outlet air temperatures, and Figure 5b illustrates the temperature variations. The maximum outlet air temperatures reached 58.5°C and 57°C, with maximum temperature differences of 42°C and 36.4°C for the two water flow rates, respectively. The data demonstrate that changing the water mass flow rate has minimal effect on the outlet air temperature, as the heat exchange primarily involves water, PCM(PCM), PM(PM), and metal plates. Possible explanation: This limited effect can be attributed to the constant air flow rate and the thermal insulation of the system, which reduces the influence of water flow variations on the outlet air temperature.

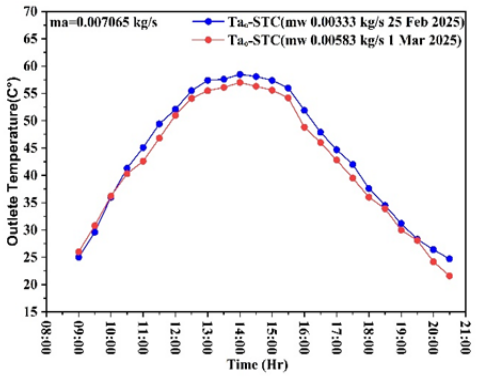

(a)

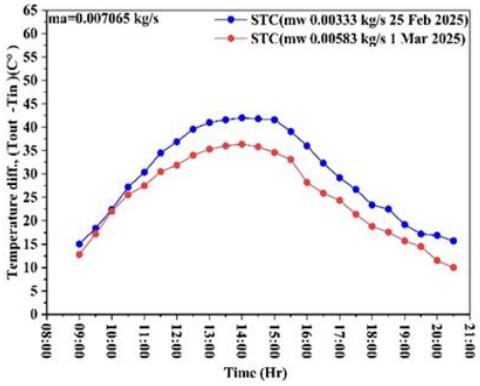

(b)

Fig.5. The difference between incoming and outgoing air temperatures. (a) Outgoing air temperature for two days. (b) Difference in air temperature for two days.

3.4. Electrical Efficiency and The Electrical Power Output of PVT

Figure 6 illustrates the variations in experimentally generated electrical power, photovoltaic (PV) cell efficiency, and cell temperatures over two consecutive test days. The photovoltaic-thermal (PVT) system exhibited a performance behavior clearly linked to changes in solar irradiance and cooling conditions. The system's electrical output increased significantly between 9:00 a.m. and 1:00 p.m., coinciding with the peak solar irradiance, then gradually decreased in the afternoon, reaching its minimum at 5:00 p.m. On February 25 and March 1, the system achieved maximum electrical outputs of 136.14 W and 142.69 W, respectively, with water mass flow rates of 0.00333 and 0.00583 kg/s. The corresponding electrical efficiencies were 11.48% and 12.22%, indicating the positive effect of higher water flow rates on enhancing cooling and improving electrical efficiency. No mechanical pump was used to circulate water; instead, a 3-meter-high water tank provided water flow by gravity. Additionally, the entire electrical energy generated was used for household consumption to compensate for the energy required by the air blower in the solar thermal (ST) collector, and this consumption was not included in the experimental energy output calculations. It should be noted that the two open-loop systems (PVT and ST) were connected only via water flow, while air flow was limited to the ST system, which operates under an open exhaust configuration. Water proved effective as a cooling medium for the PV cells, as higher flow rates enhanced heat removal from the cell surface, resulting in lower cell temperatures and improved efficiency. Figure 6-c shows that the PV cell temperature curve is inversely related to the electrical efficiency curve, since higher cell temperatures increase internal resistance, reducing the conversion efficiency of solar energy to electricity. Consequently, the combination of high solar irradiance and low water flow leads to higher cell temperatures and lower efficiency. In the morning, high irradiance levels and effective cooling maintained stable electrical power generation between 9:00 a.m. and 1:30 p.m. The initial lower cell temperatures contributed to higher electrical efficiency, which later decreased in the afternoon due to heat accumulation, before slightly improving toward the end of the day. Overall, the system's electrical efficiency showed some fluctuations due to climatic variations and operating conditions, as it depends directly on solar irradiance and PV cell area, making it sensitive to environmental changes during the test period.

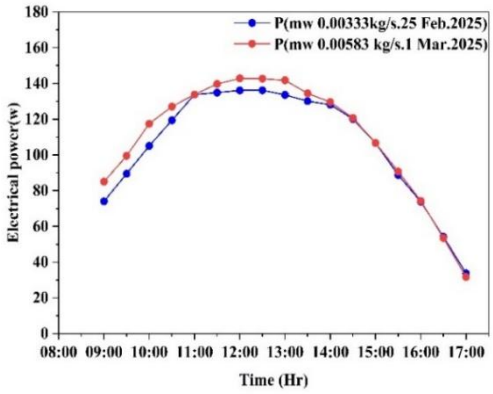

(a)

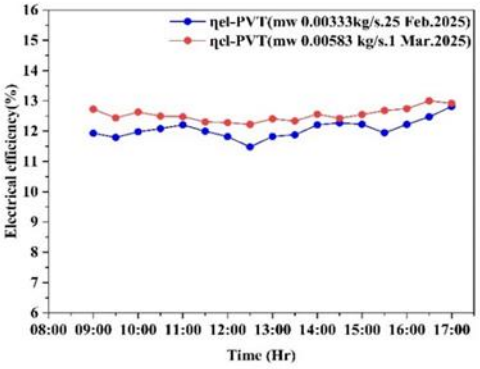

(b)

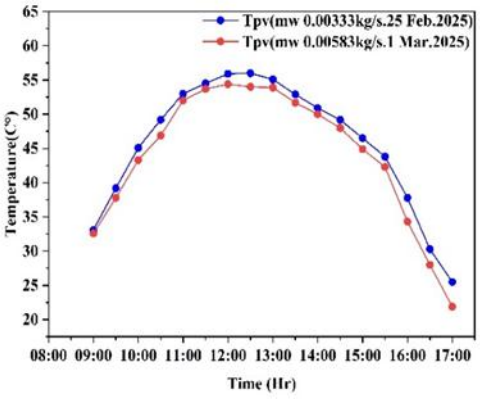

(c)

Fig.6. Variation in electrical power, electrical efficiency, and PV cell temperature in PVT. (a) electrical power. (b) electrical efficiency, (c) PV cell temperature.

3.5. Temperature of PCM, PM.

Paraffin wax (PCM) and gravel (PM) were used to investigate their impact on the performance of the solar thermal collector (ST), as these materials help extend the heating period of water and air during periods of low or absent solar irradiance. The water mass flow rate had a limited effect on the temperatures of PCM and PM, whereas air mass flow had a greater influence. Figure 7a shows the behavior of PCM over two consecutive days at a constant air flow of 0.007065 kg/s and water flow rates of 0.00333 and 0.00583 kg/s. PCM begins the day by absorbing solar radiation and gradually heating, remaining solid until approximately 13:30. Its high thermal storage capacity helps minimize temperature fluctuations. The maximum PCM temperatures reached 69.1°C and 66.7°C for the respective water flow rates. The PM acts as a sensible heat storage medium, absorbing heat faster than PCM and beginning to cool earlier. Placing PM above the absorber plate increases the surface area available for heat exchange, extending the heating duration of water and air within the system. PM temperatures are slightly affected by air and water flow rates, with maximum temperatures of 67°C and 65.5°C for water flow rates of 0.00333 and 0.00583 kg/s, respectively. These results indicate that PCM and PM together form an integrated thermal storage system, capable of storing solar energy during the day and releasing it when irradiance decreases, thereby enhancing the heating of water and air during daytime and after sunset and improving the generation of hot air exiting the system.

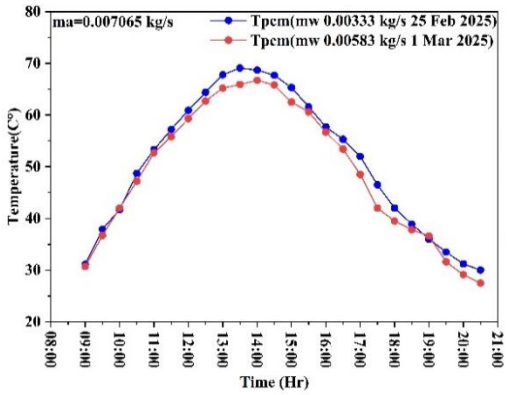

(a)

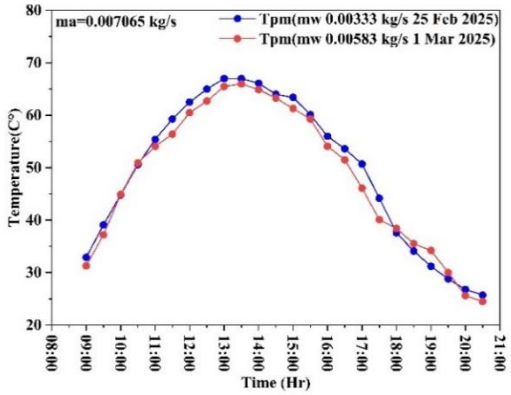

(b)

Fig 7. Temperature variation of PCM, PM. (a) PCM temperature. (b) PM temperature.

3.6. Heat Gained in PVT-ST

A performance analysis of the PVT-ST air–water system was conducted under various operating conditions to investigate the effects of different water mass flow rates, while maintaining an air mass flow rate of 0.007065 kg/s during the ST system test days. Figure 8a shows the heat energy gained by the water and air in the ST system, while Figure 8b presents the total thermal energy of the PVT-ST system, which includes the contribution from the water-based PVT system in addition to the water-based ST system. It was observed that increasing the water mass flow reduces the temperature variation of the water within the collector, as well as the temperature change of the outlet water; however, a higher water mass leads to a greater accumulation of thermal energy. The results indicate that increasing the flow rate is not the only factor enhancing thermal energy gain. Thermal storage materials, such as (PCM) and porous media, play a significant role by extending the heating duration of water and air within the solar thermal collector, thereby increasing the heat energy gained even under low or absent solar radiation, which enhances the overall thermal efficiency of the system. The ST system recorded a maximum thermal energy of 536.66 W at a water mass flow of 0.00583 kg/s and 493.31 W at a flow of 0.00333 kg/s, with the air mass flow maintained as mentioned. The peak values were recorded after 13:30, primarily due to the effect of the thermal storage materials. For the PVT-ST system, the results showed that increasing the water mass flow along with integrating thermal storage materials led

to a higher total thermal energy gain and reduced temperature differences in both water and air. The system achieved a maximum total thermal energy of 756.13 W at 0.00583 kg/s and 677.36 W at 0.00333 kg/s, demonstrating that optimizing the water mass flow in combination with thermal storage materials effectively enhances the system's thermal efficiency

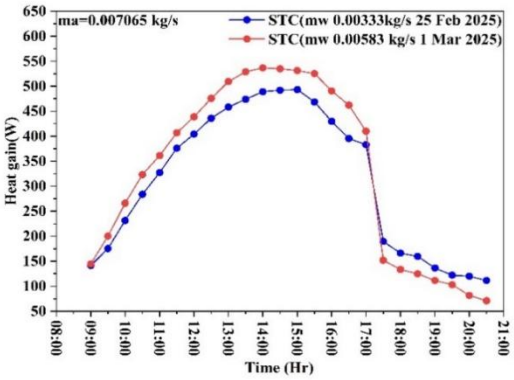

(a)

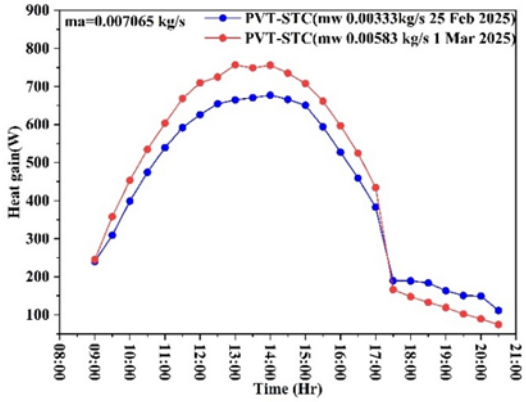

(b)

Fig.8.Variation in thermal energy output for four water mass flow rates and a constant air mass flow rate for days (25 Feb,1 Mar 202) in PVT-ST. (a) thermal energy of(air-water) in ST. (b)Total thermal energy in PVT-ST.

3.7. Thermal efficiency

Figure 9-a illustrates the changes in the thermal efficiency of the hybrid PVT–ST solar collector system over the test period, measured at half-hour intervals. The thermal performance of the water and air paths within the ST collector unit was evaluated using variable water flow rates and constant air flow over two days. The results revealed exceptionally high instantaneous thermal efficiencies for both water and air, reaching 245% and 213%, respectively, at water flow rates ranging from 0.00333 to 0.00583 kg/s. These high values can be attributed to the integration of thermal storage materials within the system, including phase change materials (PCM) and a porous medium. These materials store thermal energy during periods of high solar radiation and gradually release it when solar input decreases, allowing continued heating of water and air even after direct solar irradiation declines. By observing Figure 4, which shows the variation in water temperature, and Figure 5b, which shows the variation in air temperature, it is evident that the system continues to gain thermal energy toward the end of the day. Consequently, during periods of low instantaneous solar radiation—particularly in the late afternoon—the thermal energy output of the system can temporarily exceed the instantaneous solar input, resulting in efficiencies greater than 100%. The relatively small collector area and low solar radiation during the final measurement intervals further amplify this effect. It was also observed that the thermal energy of the solar thermal collector was high at the end of the day, which led to high thermal efficiency when considering the energy gained at the end of the day relative to the low solar radiation during the same period. This is clearly shown when reviewing Figure 8, which represents the solar energy, and Figure 3, which represents the solar irradiance, indicating an increase in the collector's thermal energy despite the low instantaneous solar input, thereby enhancing the instantaneous thermal efficiency at the end of the day. The overall thermal efficiency of the system is calculated as the sum of all thermal energy gained by both water and air divided by the product of instantaneous solar irradiance and the total collector area. Specifically, the thermal efficiency of the solar thermal (ST) collector is defined as the sum of the thermal energy gained by water and air divided by the product of instantaneous solar irradiance and the ST collector area, which in this study is 0.75 m². Figure 9 also shows that the overall thermal efficiency gradually increases over time and is higher at elevated water flow rates, reflecting improved heat transfer and reduced thermal losses. The highest overall thermal efficiency was recorded at 17:00 on both days, reaching 86% and 110.6%,

respectively. It was observed that the individual thermal efficiency of the ST unit and the overall efficiency of the combined PVT–ST system were lower than the combined thermal efficiency of water and air alone, because the overall efficiency is calculated based on the total area of both the PVT and ST collectors. This distribution of heat over a larger area reduces the relative efficiency value, although the difference remains limited. The exceedance of 100% in instantaneous thermal efficiency does not violate thermodynamic principles, as it reflects the release of stored energy in addition to the instantaneous solar input. When considering cumulative efficiency over the full test period, the system's performance remains within physically plausible limits, confirming the effectiveness of PCM and the porous medium in enhancing heat retention and maintaining thermal output even under reduced solar radiation conditions.

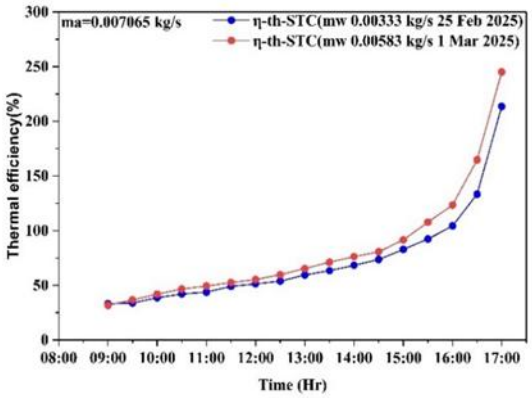

(a)

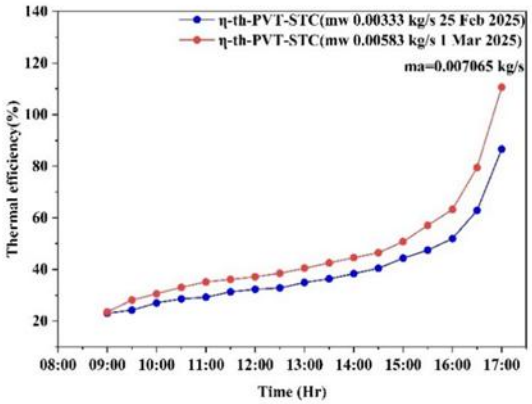

(b)

Fig.9. Variation in thermal efficiency of PVT-ST with two water mass flow rate and constant air mass flow rate. (a) thermal efficiency of combined air-water ST. (e) Total thermal efficiency of the PVT-ST system.

4. Comparison

Table 5: Comparison Between the Present Study and Previous Related Works

Study/	Study Type	Findings	Difference from Present Study
Kazemian et al. [13]	Numerical	thermal efficiency 56.55%	No PCM/PM, no air–water integration
Ma et al. [14]	Numerical	Stable electrical output,	No PCM/PM, no ST or air coupling
Li et al. [15]	Numerical	energy eff. 41.51%, exergy 17.63%	No PCM/PM, no air–water system
Salman et al. [16]	Experimental	PV temp reduced by 9–14°C	No PCM, no PVT–ST integration
Altharwanee et al. [21]	Experimental	Thermal efficiency increase, improved hot-water	No PCM/PM, no dual-fluid system
Present Study (2025)	Experimental	Air temp up to 58°C; η_{ele} =11.5–12.2%; total thermal output 756 W	First experimental PVT–ST air–water system using both PCM + PM together

5. Conclusion

This study evaluated the thermal and electrical performance of a water-based PVT system integrated with a water-based ST collector, highlighting the role of phase change materials (PCMs) and porous media (PM) in enhancing heat retention

1. The integrated PVT–ST system effectively heats water and air while generating electricity, with PCMs and PMs prolonging heat retention during low solar radiation periods.

2. Lower water flowrates increase fluid temperatures, while higher flow rates improve heat transfer and reduce temperature fluctuations.

3. Electrical performance is optimized at suitable water flow rates, balancing panel temperature and power output.

4. Overall efficiency improves with higher water and air flow rates, confirming the effectiveness of the integrated PVT–ST design.

Overall, the results demonstrate that integrating PVT and ST systems with thermal storage materials can significantly enhance energy capture and utilization, providing a practical approach for efficient solar energy systems.

References

[1] M. M. M. Salih, O. R. Alomar, F. A. Ali, and H. M. Abd, "An experimental investigation of a double pass solar air heater performance: A comparison between natural and forced air circulation processes," Sol. Energy, vol. 193, pp. 184–194, Nov. 2019, doi: 10.1016/j.solener.2019.09.060.

[2] H. N. S. Yassien, O. R. Alomar, and M. M. M. Salih, "Performance analysis of triple-pass solar air heater system: Effects of adding a net of tubes below absorber surface," Sol. Energy, vol. 207, pp. 813–824, Sep. 2020, doi: 10.1016/j.solener.2020.07.041.

[3] M. M. M. Salih, O. R. Alomar, and H. N. S. Yassien, "Impacts of adding PMon performance of double-pass solar air heater under natural and forced air circulation processes," Int. J. Mech. Sci., vol. 210, no. May, p. 106738, 2021, doi: 10.1016/j.ijmecsci.2021.106738.

[4] H. M. Abd, O. R. Alomar, F. A. Ali, and M. M. M. Salih, "Experimental Study of Compound Parabolic Concentrator with Flat Plate Receiver," Appl. Therm. Eng., p. 114678, 2019, doi: 10.1016/j.applthermaleng.2019.114678.

[5] O. R. Alomar and O. M. Ali, "Energy and exergy analysis of hybrid photovoltaic thermal solar system under climatic condition of North Iraq," Case Stud. Therm. Eng., vol. 28, no. May, p. 101429, 2021, doi: 10.1016/j.csite.2021.101429.

[6] E. Vengadesan and R. Senthil, "A review on recent development of thermal performance enhancement methods of fl at plate solar water heater," Sol. Energy, vol. 206, no. April, pp. 935–961, 2020, doi: 10.1016/j.solener.2020.06.059.

[7] M. Patil, A. Sidramappa, S. Kumar, and A. M. Hebbale, "Materials Today: Proceedings Experimental study of solar PV / T panel to increase the energy conversion efficiency by air cooling," Mater. Today, Proc., vol. 92, pp. 309–313, 2023, doi: 10.1016/j.matpr.2023.05.007.

[8] A. Kazemian, A. Parcheforosh, A. Salari, and T. Ma, "Optimization of a novel photovoltaic thermal module in series with a solar collector using Taguchi based grey relational analysis," Sol. Energy, vol. 215, no. November 2020, pp. 492–507, 2021, doi: 10.1016/j.solener.2021.01.006.

[9] H. S. Xue, "Experimental investigation of a domestic solar water heater with solar collector coupled phase-change energy storage," Renew. Energy, vol. 86, pp. 257–261, Feb. 2016, doi: 10.1016/j.renene.2015.08.017.

[10] R. Kansara, M. Pathak, and V. K. Patel, "International Journal of Thermal Sciences Performance assessment of flat-plate solar collector with internal fins and PMthrough an integrated approach of CFD and experimentation," Int. J. Therm. Sci., vol. 165, no. March, p. 106932, 2021, doi: 10.1016/j.ijthermalsci.2021.106932.

[11] P. Jha, B. Das, R. Gupta, J. D. Mondol, and M. A. Ehyaei, "Review of recent research on photovoltaic thermal solar collectors Solar thermal," vol. 257, no. April, pp. 164–195, 2023.

[12] M. Valizadeh, F. Sarhaddi, and M. Adeli, "Exergy performance assessment of a linear parabolic trough photovoltaic thermal collector," Renew. Energy, vol. 138, pp. 1028–1041, 2019, doi: 10.1016/j.renene.2019.02.039.

[13] A. Kazemian, A. Salari, T. Ma, and H. Lu, "Application of hybrid nanofluids in a novel

combined photovoltaic / thermal and solar collector system," Sol. Energy, vol. 239, no. January, pp. 102–116, 2022, doi: 10.1016/j.solener.2022.04.016.

[14] T. Ma, M. Li, and A. Kazemian, "Photovoltaic thermal module and solar thermal collector connected in series to produce electricity and high-grade heat simultaneously," Appl. Energy, vol. 261, no. October 2019, p. 114380, 2020, doi: 10.1016/j.apenergy.2019.114380.

[15] M. Li, D. Zhong, T. Ma, A. Kazemian, and W. Gu, "Photovoltaic thermal module and solar thermal collector connected in series: Energy and exergy analysis," Energy Convers. Manag., vol. 206, Feb. 2020, doi: 10.1016/j.enconman.2020.112479.

[16] A. H. A. Salman, K. H. Hilal, and S. A. Ghadhban, "Enhancing performance of PV module using water flow through porous media," Case Stud. Therm. Eng., vol. 34, p. 102000, Jun. 2022, doi: 10.1016/j.csite.2022.102000.

[17] Z. Han, K. Liu, G. Li, X. Zhao, and S. Shittu, "Electrical and thermal performance comparison between PVT-ST and PV-ST systems," Energy, vol. 237, p. 121589, 2021, doi: 10.1016/j.energy.2021.121589.

[18] G. S. Menon, S. Murali, J. Elias, D. S. A. Del, P. V Al, and M. P. Samuel, "Experimental investigations on unglazed photovoltaic-thermal (PVT) system using water and nano fl uid cooling medium," vol. 188, 2022, doi: 10.1016/j.renene.2022.02.080.

[19] V. Suresh, S. Iqbal, K. S. Reddy, and B. Pesala, "3-D numerical modelling and experimental investigation of coupled photovoltaic thermal and flat plate collector," Sol. Energy, vol. 224, no. June, pp. 195–209, 2021, doi: 10.1016/j.solener.2021.05.079.

[20] A. Hmoud, M. Kazemi, and H. Soroush, "Enhanced performance of photovoltaic thermal module and solar thermal flat plate collector connected in series through integration with phase change materials : A comparative study," Therm. Sci. Eng. Prog., vol. 47, no. October 2023, p. 102305, 2024, doi: 10.1016/j.tsep.2023.102305.

[21] H. Altharwanee, F. Jurado, and D. Vera, "Experimental study on the performance of the photovoltaic thermal (PVT) connected in series with flat plate solar collector (ST)," Sol. Energy, vol. 283, no. July, p. 113010, 2024, doi: 10.1016/j.solener.2024.113010.

[22] M. A. Basim and O. Rafae, "Impacts of Adding PMand Phase Change Material on Performance of Solar Water Distiller System Under Iraq Climatic Condition : An Experimental Study," 2024, doi: 10.1002/est2.70038.

[23] M. Nazaer, O. Rafae, and A. Mustafa, "Performance of compound parabolic concentrator solar air flat plate collector using phase change material," Appl. Therm. Eng., vol. 240, no. August 2023, p. 122224, 2024, doi: 10.1016/j.applthermaleng.2023.122224.

[24] M. N. Yousif, A. M. Saleem, and O. R. Alomar, "Development of Compound Parabolic Concentrator based on Flat Plate Receiver Solar Air Heater and Phase Change Material," vol. 6, no. 2023, pp. 1–9, 2024.

[25] A. M. A. Morad, A. K. S. Al-sayyab, and M. A. Abdulwahid, "Case Studies in Thermal Engineering Optimisation of tilted angles of a photovoltaic cell to determine the maximum generated electric power : A case study of some Iraqi cities," Case Stud. Therm. Eng., vol. 12, no. July, pp. 484–488, 2018, doi: 10.1016/j.csite.2018.07.001.

[26] Q. Hassan, M. K. Abbas, A. M. Abdulateef, J. Abdulateef, and A. Mohamad, "RETRACTED: Assessment the potential solar energy with the models for optimum tilt angles of maximum solar irradiance for Iraq," Case Stud. Chem. Environ. Eng., vol. 4, p. 100140, 2021, doi: 10.1016/j.cscee.2021.100140.

[27] L. Xu et al., "A hybrid PV thermal (water or air) wall system integrated with double air channel and phase change material : A continuous full-day seasonal experimental research," Renew. Energy, vol. 173, pp. 596–613, 2021, doi: 10.1016/j.renene.2021.04.008.

[28] M. Emam, A. Hamada, H. A. Refaey, M. Moawed, M. A. Abdelrahman, and M. R. Rashed,

"Year-round experimental analysis of a water-based PVT-PCM hybrid system: Comprehensive 4E assessments," Renew. Energy, vol. 226, p. 120354, May 2024, doi: 10.1016/j.renene.2024.120354.

[29] Z. Arifin et al., "ScienceDirect The application of TiO 2 nanofluids in photovoltaic thermal collector systems," Energy Reports, vol. 8, no. May, pp. 1371–1380, 2022, doi: 10.1016/j.egyr.2022.08.070.

[30] D. L. Bätzner et al., "Properties of high efficiency silicon heterojunction cells," Energy Procedia, vol. 8, no. April, pp. 153–159, 2011, doi: 10.1016/j.egypro.2011.06.117.

[31] A. Salari, A. Taheri, A. Farzanehnia, M. Passandideh-fard, and M. Sardarabadi, "An updated review of the performance of nanofluid-based photovoltaic thermal systems from energy, exergy, economic, and environmental (4E) approaches," 2020, doi: https://doi.org/10.1016/j.jclepro.2020.124318.

[32] A. S. Abdullah, M. M. A. Al-sood, Z. M. Omara, M. A. Bek, and A. E. Kabeel, "Performance evaluation of a new counter fl ow double pass solar air heater with turbulators," Sol. Energy, vol. 173, no. July, pp. 398–406, 2018, doi: 10.1016/j.solener.2018.07.073.

[33] E. Vengadesan, D. Bharathwaj, B. S. Kumar, and R. Senthil, "Experimental study on heat storage integrated flat plate solar collector for combined water and air heating in buildings," Appl. Therm. Eng., vol. 216, no. July, p. 119105, 2022, doi: 10.1016/j.applthermaleng.2022.119105.

[34] A. Kazemian, M. Hosseinzadeh, and M. Sardarabadi, "E ff ect of glass cover and working fl uid on the performance of photovoltaic thermal (PVT) system : An experimental study," vol. 173, no. June 2017, pp. 1002–1010, 2018, doi: 10.1016/j.solener.2018.07.051.

[35] A. Kazemian, A. Salari, and T. Ma, "A year-round study of a photovoltaic thermal system integrated with phase change material in Shanghai using transient model," Energy Convers. Manag., vol. 210, no. February, p. 112657, 2020, doi: 10.1016/j.enconman.2020.112657.

[36] J. P. Holman, "Experimental methods for engineers," 1966.

Nomenclature

ST	Solar Thermal Collector
PV	Photovoltaic
PVT	Photovoltaic Thermal
PVT-ST	Photovoltaic Thermal Connected with solar thermal collector
η_{el}	Electrical efficiency
$\boldsymbol{P_{max}}$	Electrical power (W)
G	The intensity of solar radiation (W/m^2)
I	solar panel- current (A)
V	solar panel- voltage (V)
$\dot{m}$	Mass flow rate (kg/s)
$\boldsymbol{Q_w}$	Water heat gain (W)
$\boldsymbol{Q_a}$	Air heat gain (W)
ρ	Air density (kg/m^3)
$\boldsymbol{Q_u}$	Total heat gain in ST(W)
$\boldsymbol{\dot{Q}_{th}}$	Total heat gain in PVT-ST(W)
PCM	Phase change materials
PM	Porous medium
A_d	Area of the duct (m²)
$\boldsymbol{V_d}$	Air velocity(m/s)